Optimally Conditioned Channel Matrices in Precoding Enabled Non-Terrestrial Networks

Jevgenij Krivochiza, Hong-fu Chou, J.C. Merlano-Duncan, Symeon Chatzinotas

SnT - securityandtrust.lu, University of Luxembourg, Luxembourg
Email: {jevgenij.krivochiza, hungpu.chou, juan.duncan, symeon.chatzinotas}@uni.lu

***Abstract*—This paper explores how the condition number of the channel matrix affects the performance of different precoding techniques in non-terrestrial network (NTN) communications. Precoding is a technique that can improve the signal-to-interference-plus-noise ratio (SINR) and bit error rate (BER) in massive multi-beam systems. However, the performance of precoding depends on the rank and condition number of the channel matrix, which measures how well-conditioned the matrix is for inversion. We compare three precoding techniques: zero-forcing (ZF), minimum mean square error (MMSE), and semi-linear precoding (SLP), and show that their performance degrades as the condition number increases. To mitigate this problem, we propose a user ordering approach that forms optimally conditioned channel matrices by selecting users with orthogonal channel vectors. We demonstrate that this approach improves the SINR and goodput of all the precoding techniques in full-frequency reuse NTN communications.**

***Index Terms*—Multiuser MISO, Symbol-level precoding, user ordering, channel matrix,**

I. Introduction

Non-terrestrial network (NTN) communications are emerging as a promising technology for beyond 5G (B5G) applications, as they can provide wide-area coverage and service availability over untapped or underserved geographic areas [1]. NTN communications rely on multi-layer space platforms, such as satellites and high-altitude platforms, to support various types of connections that may be made anywhere and at any time [2]. In order to fulfill the demands of connections that may be made anywhere and at any time, an NTN is designed to offer wide-area coverage while ensuring service availability and scalability [3]. Moreover, NTN communications can ensure service continuity in mission-critical scenarios that cannot tolerate failures, such as disaster relief or emergency response, where terrestrial communications may be disrupted by natural catastrophes or terrorism [4].

One of the key challenges in NTN communications is to improve the spectral efficiency and reliability of massive multi-beam systems, where multiple users share the same frequency band and interfere with each other. Precoding is a technique that can enhance the performance of these systems by pre-processing the transmitted signals at the transmitter side to mitigate the interference and improve the signal-to-interference-plus-noise ratio (SINR) and bit error rate (BER) at the receiver side [5]–[7].

Many studies have demonstrated various precoding enabled system designs for NTN communications in [8]–[10]. In [11], [12] we demonstrated a complete end-to-end test-bed for precoding validation over a live satellite link using the DVB-S2X framework [13].

The effectiveness of precoding depends on the rank and condition number of the channel matrix, which measures how well-conditioned the matrix is for inversion. A high condition number indicates a poorly conditioned matrix that can degrade the performance of precoding techniques such as zero-forcing (ZF), minimum mean squared error (MMSE), and symbol-level precoding (SLP). Previous studies in [5], [14] and [15] have proposed user ordering techniques for precoding, but they did not provide a closed-form solution or establish a clear relation between the condition number and the precoding performance. In [16], [17] different user ordering techniques were developed tailored for specific precoding techniques.

In this work, we address these gaps by investigating how different channel matrix configurations affect the SINR and goodput of ZF, MMSE, and SLP precoders. We also propose a user ordering approach that forms optimally conditioned channel matrices by selecting users with orthogonal channel vectors. We demonstrate that our approach improves the performance of all the precoding techniques in full-frequency reuse NTN communications.

Notation: Upper-case and lower-case bold-faced letters are used to denote matrices and column vectors. The superscripts $(\cdot)^H$, $(\cdot)^\dagger$ and $(\cdot)^{-1}$ represents Hermitian matrix, matrix transpose and inverse operations. $\|\cdot\|_2$ is the Euclidean norm, $|\cdot|$ is an absolute magnitude of a complex value. The real and imaginary parts of a complex value are defined as $\mathrm{Re}(\cdot)$ and $\mathrm{Im}(\cdot)$. The imaginary unit is denoted as $\imath$. Square diagonal matrices are denoted as $\mathbf{diag}[\cdot]$ with the elements defined on their main diagonal. Identity $n \times n$ matrix is defined as $\mathbf{I}_n$

II. Matrix Condition Number Impact on Precoding

A. System Model

We consider a system model with the forward link of a multiuser multi-antenna wireless communication system. We assume the system to use the full frequency reuse scenario, in which all the antennas transmit in the same frequency and

This work was supported by the Luxembourg National Research Fund under the Industrial Partnership Block Grant (IPBG) – TeRrestrial Systems for Ubiquitous Beyond 5G CommunicaTions (INSTRUCT) Nr. IPBG19/14016225/INSTRUCT

time. The multi-user interference is managed using precoding. We define the number of the transmitting antennas as N_t and the total number of single-antenna user terminals (UTs) as N_u in the coverage area. In the specified MU-MIMO channel model, the received signal at the i-th UT is given by $y_i = \mathbf{h}_i^\dagger \mathbf{x} + u_i + n_i$, where $\mathbf{h}_i^\dagger$ is a $1 \times N_t$ vector representing the complex channel coefficients between the i-th UT and the N_t antennas of the transmitter, $\mathbf{x}$ is defined as the $N_t \times 1$ vector of the transmitted symbols at a certain symbol period, u_i is a constructive interference component of SLP precoding, and n_i is the independent complex circular symmetric (c.c.s.) independent identically distributed (i.i.d) zero mean Additive White Gaussian Noise (AWGN) measured at the i-th terminal's receive antenna.

Looking at the concatenated formulation of the received signal, which includes the whole set of receiver terminals, the linear signal model is

$$\mathbf{y} = \mathbf{H}\mathbf{x} + \mathbf{n} = \mathbf{H}\mathbf{W}(\mathbf{s} + \mathbf{u}) + \mathbf{n}, \tag{1}$$

where $\mathbf{y} = [y_1, y_2, \ldots, y_i] \in \mathbb{C}^{N_u \times 1}$, $\mathbf{n} = [n_1, n_2, \ldots, n_i] \in \mathbb{C}^{N_u \times 1}$, $\mathbf{x} \in \mathbb{C}^{N_t \times 1}$, $\mathbf{s} \in \mathbb{C}^{N_u \times 1}$, $\mathbf{u} = [u_1, u_2, \ldots, u_i] \in \mathbb{C}^{N_u \times 1}$ and $\mathbf{H} = [\mathbf{h}_i^\dagger, \mathbf{h}_i^\dagger, \ldots, \mathbf{h}_i^\dagger] \in \mathbb{C}^{N_u \times N_t}$. We define a precoding matrix $\mathbf{W} \in \mathbb{C}^{N_t \times N_u}$ which maps the information symbols $\mathbf{s}$ into precoded symbols $\mathbf{x}$. We consider the data symbols $\mathbf{s}$ to be unit variance complex vectors $|s_i| = 1$ for every $i = 1, 2, \ldots, N_u$. The vector $\mathbf{u}$ represent the constructive interference in the received symbols of all the users. The precoding matrix $\mathbf{W}$ and the vector $\mathbf{u}$ are defined accordingly to the selected precoding technique, which we describe in the following section.

B. Precoding Techniques

1) Channel Inversion: We define the precoding matrix $\mathbf{W}_{\mathrm{ZF}}$ as the ZF precoder:

$$\mathbf{W}_{\mathrm{ZF}} = \mathbf{H}^H(\mathbf{H}\mathbf{H}^H)^{-1}/f_{\mathrm{ZF}}, \tag{2}$$

where $f_{\mathrm{ZF}} = \sqrt{\sum_{n=1}^{N_t}\sum_{m=1}^{N_u} \mathbf{W}_{\mathrm{ZF}}{}^2_{n,m}}$ is a rescaling factor to account for sum power constraints. In this case $u_i = 0$ for all $i = 1, 2, \ldots, N_u$.

2) Regularized Channel Inversion: We define the precoding matrix ($\mathbf{W}$) as the MMSE precoder:

$$\mathbf{W}_{\mathrm{MMSE}} = \mathbf{H}^H(\mathbf{H}\mathbf{H}^H + \sigma^2\mathbf{I}_{N_U})^{-1}/f_{\mathrm{MMSE}}, \tag{3}$$

where $f_{\mathrm{MMSE}} = \sqrt{\sum_{n=1}^{N_t}\sum_{m=1}^{N_u} \mathbf{W}_{\mathrm{MMSE}}{}^2_{n,m}}$ is a rescaling factor to account for the sum power constraints, σ^2 - noise variance at the UTs. In this case $u_i = 0$ for all $i = 1, 2, \ldots, N_u$.

3) Symbol-Level Precoding: We define symbol-level precoding (SLP) as in [18]. The following optimization problem is devoted:

$$\begin{aligned} \min_{\tilde{\mathbf{u}}} \quad & \|\widehat{\mathbf{W}}_{\mathrm{ZF}}(\tilde{\mathbf{s}} + \tilde{\mathbf{u}})\|_2 \\ s.t. \quad & \tilde{u}_k \geq 0, \end{aligned} \tag{4}$$

for all $k = 1, 2, \ldots 2N_u$, $\widehat{\mathbf{W}}_{\mathrm{ZF}} = [\mathrm{Re}(\mathbf{W}_{\mathrm{ZF}}\mathbf{B}), -\mathrm{Im}(\mathbf{W}_{\mathrm{ZF}}\mathbf{B}); \mathrm{Im}(\mathbf{W}_{\mathrm{ZF}}\mathbf{B}), \mathrm{Re}(\mathbf{W}_{\mathrm{ZF}}\mathbf{B})] \in \mathbb{R}^{2N_t \times 2N_u}$, $\tilde{\mathbf{s}} = [|\mathrm{Re}(s_1)|, |\mathrm{Re}(s_2)|, \ldots, |\mathrm{Re}(s_{N_u})|, |\mathrm{Im}(s_1)|, |\mathrm{Im}(s_2)|, \ldots, |\mathrm{Im}(s_{N_u})|] \in \mathbb{R}^{2N_u \times 1}$, and $\tilde{\mathbf{u}} = [|\mathrm{Re}(u_1)|, |\mathrm{Re}(u_2)|, \ldots, |\mathrm{Re}(u_{N_u})|, |\mathrm{Im}(u_1)|, |\mathrm{Im}(u_2)|, \ldots, |\mathrm{Im}(u_{N_u})|] \in \mathbb{R}^{2N_u \times 1}$. There are additional constraints for $\tilde{u}_k$ in the [18]. We ignore these constrains in this work, as they are required only for QAM constellations with modulation order higher than 4. For simplicity, we use 4-QAM symbols in all the benchmarks.

The matrix $\mathbf{B}$ represents the rotation of the symbol vectors into the first quadrature of the complex plane and is defined as

$$\mathbf{B} = \mathbf{diag}\begin{bmatrix} b_1, & b_2, & \ldots, & b_i \end{bmatrix}. \tag{5}$$

$$b_i = \begin{cases} 1 & \text{if } \mathrm{Re}(s_i) > 0 \text{ and } \mathrm{Im}(s_i) > 0 \\ \iota 1 & \text{if } \mathrm{Re}(s_i) < 0 \text{ and } \mathrm{Im}(s_i) > 0 \\ -\iota 1 & \text{if } \mathrm{Re}(s_i) > 0 \text{ and } \mathrm{Im}(s_i) < 0 \\ -1 & \text{if } \mathrm{Re}(s_i) < 0 \text{ and } \mathrm{Im}(s_i) < 0 \end{cases}, \tag{6}$$

for $i = 1, 2, \ldots, N_u$. The following equality is therefore respected

$$\mathbf{s} = \mathbf{B}\tilde{\mathbf{s}}. \tag{7}$$

The problem (4) is a non-negative least squares (NNLS) problem. It can be solved using Fast NNLS algorithm developed in [19]. In this case $\mathbf{u}$ is the output of the Fast NNLS algorithm.

C. SINR Estimation

To evaluate the performance, we consider signal-to-interference-plus-noise ratio (SINR) estimation measured on the actual pilots at the UT side rather than using SINR estimation based on the precoding matrix [20]. SINR estimation is suitable for SLP techniques, where SINR depends on both the precoding matrix and the symbol constructive interference. The authors in [21] showed that estimating SINR at the UT side is more reliable than SINR calculated at the gateway side. The DVB-S2 standard uses the Signal-to-Noise Ratio Estimation (SNORE) algorithm [22]. The SNORE algorithm work in data-aided (DA) operating mode. The pilot presence allows to use the DA version of the SNORE algorithm operating on the pilot time slots and therefore we insert pilots into the beginning of transmitted frames for each user. The pilot sequence for i-th UT is generated as in [13] part E.3.5.3. The pilot fields are determined by a Walsh-Hadamard (WH) sequence of size 32 plus padding of a Walsh-Hadamard (WH) sequence of size 16. A set of $2^5 = 32$ orthogonal WH sequences results from the following recursive construction principle:

$$\mathbf{P}_m = \begin{bmatrix} \mathbf{P}_{m-1} & \mathbf{P}_{m-1} \\ \mathbf{P}_{m-1} & -\mathbf{P}_{m-1} \end{bmatrix}, \tag{8}$$

starting from $m > 1$ and $\mathbf{P}_1 = 1$ until $\mathbf{P}_{32}$ is denoted. The i-th row of $\mathbf{P}_{32}$ corresponds to the i-th WH sequence with $i = 1, \ldots, 32$. For the sake of padding, a matrix of size 32×16 is appended. This matrix is generated from $\mathbf{P}_{16}$ by repeating $\mathbf{P}_{16}$ vertically to get:

$$\mathbf{P}_{\text{padding}} = \begin{bmatrix} \mathbf{P}_{16}; \mathbf{P}_{16} \end{bmatrix}. \tag{9}$$

Putting both matrices together yields:

$$\mathbf{P}_{\text{pilot3}} = \left[\mathbf{P}_{32}; \mathbf{P}_{\text{padding}}\right], \tag{10}$$

hosting the whole set of possible pilot sequences row by row. The selection of i is a static choice for the transmit signal, thus we transmit i-th sequence to the i-th UT. The pilot sequences are multiplied by $(1+\imath)\sqrt{2}$ to generate complex symbols.

At each UT, SINR is calculated as follows:

$$\frac{E_b}{N_0} = \frac{P_S}{P_N}\frac{1}{\log_2 4}, \tag{11}$$

where P_S - power of the intended signal and P_N - power of noise plus interference. We calculate P_s as

$$P_S = \frac{1}{48}|\sum_{t=1}^{48} y_i[t] * P_{\text{pilot3}_i}[t]|^2 \tag{12}$$

We calculate P_N from the total signal power

$$P_N = P_R - P_S, \tag{13}$$

where $P_R = \frac{1}{48}\sum_{t=1}^{48}|y_i[t]|^2$.

D. Generating Channel Matrices

We consider a MU-MISO system, which has an equal number of the transmit and receive antennas $N_t = N_u = 16$. We accordingly generate a full rank $N \times N$ MU-MISO channel matrix with i.i.d. complex values. If the condition number of the matrix is very large, then the matrix is said to be ill-conditioned. Practically, such a matrix is almost singular, and the computation of its inverse, or solution of a linear system of equations is prone to large numerical errors. A matrix that is not invertible has condition number equal to infinity. The 2-norm matrix condition number is defined as

$$\kappa_2(\mathbf{H}) = ||\mathbf{H}||_2 \cdot ||\mathbf{H^{-1}}||_2. \tag{14}$$

The matrix condition number corresponds to the ratio of the largest singular value of that matrix to the smallest singular value. In the case of the MU-MISO system, the matrix condition number describes the power imbalance in the channel. To generate a channel matrix with random i.i.d. values and a desired condition number we calculate singular-value decomposition (SVD) [23] of the generated matrix ($\mathbf{H}$) as $\mathbf{H} = \mathbf{U\Sigma V}^\dagger$. $\mathbf{U}$ is an $N_u \times N_u$ complex unitary matrix, $\mathbf{\Sigma}$ is an $N_u \times N_t$ rectangular diagonal matrix with non-negative real numbers on the diagonal, and $\mathbf{V}$ is an $N_t \times N_t$ real or complex unitary matrix. We reconstruct $\mathbf{\Sigma}$ for its diagonal elements to monotonically increase from 1 to κ_2 as

$$\mathbf{\Sigma}_{\kappa_2} = \mathbf{diag}\left[1, \ldots, \kappa_2\right]. \tag{15}$$

The resulting channel matrix is then computed and its power is normalized as

$$\mathbf{H} = \frac{\mathbf{U\Sigma}_{\kappa_2}\mathbf{V}^\dagger}{\sqrt{\sum_{n=1}^{N_u}\sum_{m=1}^{N_t} h_{n,m}h_{n,m}^H}}. \tag{16}$$

We average the results over 50 channel matrix iterations with the condition numbers (κ_2) from 1 to 200.

E. Numerical Validation

We consider the following benchmarks to evaluate the performance of the precoding techniques under various channel matrix condition numbers: SINR ($\frac{E_b}{N_0}$), which is calculated using the SNORE algorithm at the UTs and the achieved BER score.

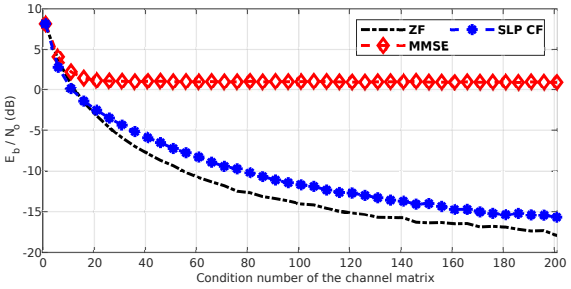

Fig. 1. Received average SNR at the UTs vs the channel matrix condition number.

The received SINR as a function of the channel matrix condition number is shown in Fig. 1. The received SINR decreases for all the benchmarked precoding techniques when the condition number increases. The ZF exhibits the most loss in SINR compared to other techniques. In the SLP case, SINR degrades less rapidly than ZF. The MMSE precoder demonstrates similar SINR dynamics in the beginning but soon reaches its optimum SINR point due to normalization in the inverse operation, which becomes more dominant in this region.

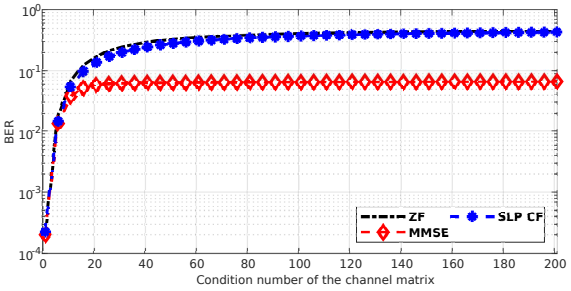

Fig. 2. Achieved BER at the UTs vs the channel matrix condition number.

We can see the achieved average BER in Fig. 2 for the same benchmark. We can see that the SINR and BER are closely related to all the techniques as would be expected. For the MMSE case, BER error is saturated near the condition number 10 as was seen for the SINR benchmark.

Fig. 3 shows the BER curves vs the achieved SINR derived from Fig. 1 and 2. We can see that SLP has a slightly lower BER in the high SINR region than ZF and MMSE techniques. In the case of the MMSE technique, the SNR range achieved during the benchmark is between 1 dB and 10 dB. We can see, that the SINR and BER performance is

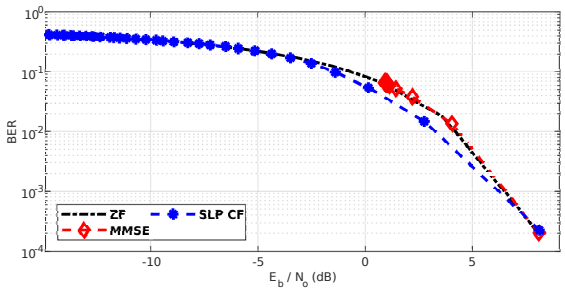

Fig. 3. Achieved BER vs the received SNR.

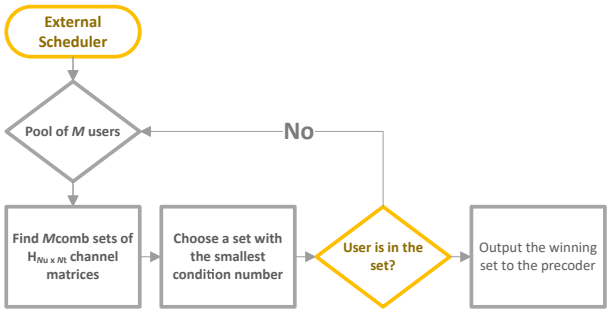

Fig. 4. Flow Diagram of the Proposed User Ordering

sensitive to the condition number of the channel matrix for all the benchmarked precoding techniques.

III. Manipulating the Condition Number of the Channel

A. Ordering Algorithm

Based on the findings, presented in the previous section, we demonstrate a user ordering algorithm to minimize the condition number of the resulting channel matrix. We consider the system has a pool of M randomly generated users, there $M > N_t$. The system serves the maximum number $N_u = N_t$ of users at any given time. For simplicity of this demonstration, we consider that the users in the pool are preselected based on the same QoS demands by the medium access control (MAC) layer of the communication system. Therefore, the ordering algorithm has no prioritization towards the users in the pool. There are M_{comb} possible permutations to order M users into sets of N_T-s. Since the order of the users in a single set does not effect the condition number so as

$$\kappa_2(h_i; h_{i+1}) = \kappa_2(h_{i+1}; h_i), \tag{17}$$

the number of possible permutations M_{comb} can be found as

$$M_{\text{comb}} = \frac{M!}{N_t!(M - N_t)!} \tag{18}$$

When the two users have a similar channel the condition number will increase towards infinity as

$$\kappa_2([h_1; h_1]) \to \infty, \tag{19}$$

which allows the ordering algorithm to avoid potentially not invertible MIMO channels in the system.

The ordering algorithm makes M_{comb} sets of $N_u \times N_t$ channels matrices and selects the one with the lowest condition number. The users, which are not in the winning set are stored back in the pool and are reconsidered in the next iterations of the algorithm when the pool is refilled with new users by the MAC layer. The users in the winning set are transferred to the precoder. The flow diagram of the proposed ordering algorithm is presented in Fig. 4.

TABLE I
Total Goodput with the Size of the User Pool M = 17

Precoding	ZF	MMSE	SLP CF
Random ordering	7949	9381	8315
Proposed ordering	8789	9434	9059
Goodput increase	10%	1%	9%

TABLE II
Total Goodput with the Size of the User Pool M = 19

Precoding	ZF	MMSE	SLP CF
Random ordering	8041	9390	8391
Proposed ordering	9222	9544	9410
Goodput increase	14%	2%	12%

B. Numerical Validation

In this benchmark, we consider a system that has $N_t = 16$ transmit antennas and the size of the user pool is $M = 17, 19$ and 21. We consider that the pool is constantly refilled with a total number of 10000 randomly generated users. The number of permutations to find a winning set in each case is 17, 969 and 20349 respectively. The number of final sets to be transmitted is 625. We can select the channel matrix from a greater number of permutations so we have more chances to get the lowest possible condition number, but it comes with the price of longer processing delays. We define the complete system goodput as

$$R = \sum_{c}^{10000} (1 - BER_c) \frac{2bits}{sHz}. \tag{20}$$

In the Table I we can see numerical results of the total achieved goodput with the proposed user ordering compared to the case without ordering (i.e. random ordering). The size of the pool is 17 in this case. We can see that all the precoders achieve the higher goodput when the proposed user ordering is applied. We get a 10% increase in terms of goodput for the ZF precoder.

In Table II we see the achieved goodput for the size of the user pool 19. Extra users in the pool give the ordering algorithm more possible perturbations to choose the best combination. We see a 14% and 12% increase of the goodput for ZF and SLP precoders. even the robust to high condition

TABLE III
TOTAL GOODPUT WITH THE SIZE OF THE USER POOL M = 21

Precoding	ZF	MMSE	SLP CF
Random ordering	8072	9398	8421
Proposed ordering	9537	9676	9649
Goodput increase	18%	3%	15%

numbers MMSE precoder demonstrates now 2% goodput increase.

In the Table III we utilize the pool of 21 users. We can see now 18% and 15% goodput increase for ZF and SLP precoders respectively. The MMSE technique improves by 3%.

Naturally, the larger is the user pool and the greater the number of possible perturbations to find a better-conditioned channel matrix, the higher results we achieve. The authors would like to note, that calculating the condition number of each possible channel matrix is a computationally expensive operation. As seen from (14), the operation involves a matrix inverse, which asymptotic complexity alone is of $O(N^3)$ for a $N \times N$ channel. This can be improved if another metric with a lower complexity is proposed to reliably detect ill-conditioned matrices. Moreover, the number of perturbation grows asymptotically with the size of the pool and results in longer calculation delays. Nevertheless, even while using the lowest user pool possible for this system, we already see improved system performance.

IV. CONCLUSION

In this paper, we demonstrated the impact of the condition number of the channel matrix on the performance of the selected precoding techniques. It was shown that if the rank of the channel matrix is fixed and its condition number is increasing, the SINR performance degrades for all the benchmarked precoding techniques, for a NTN system with a limited transmitter power. This leads to lower goodput performance at the UTs. The matrix is ill-conditioned then its condition number is high, thus the norm of the inverse of such matrix is higher. In the case of SLP, the SINR performance degrades slower than in the case of the ZF technique. On the other hand, MMSE is less sensitive to the condition number than both ZF and SLP as the technique's normalization factor is dominating in the low SINR region. We showed a closed-form algorithm to improve the channel matrix by tackling user ordering in a precoded communications system. The algorithm chooses sets of users to create channels with the lower condition number by brute-forcing though all the possible combinations of the user channel. We saw the goodput increase ranging from 1% to 18% depending on the size of the user pool and the precoding technique.

REFERENCES

[1] K. Samdanis and T. Taleb, "The road beyond 5g: A vision and insight of the key technologies," *IEEE Network*, vol. 34, no. 12, pp. 135 – 141, 2020.

[2] A. Mourad, R. Yang, P. H. Lehne, and A. D. L. Oliva, "A baseline roadmap for advanced wireless research beyond 5g," *Electronics*, vol. 9, no. 351, pp. 1–14, 2020.

[3] Y. Jiang, W. He, W. Liu, and S. Wu, "A b5g non-terrestrial-network (ntn) and hybird constellation based data collection system (dcs)," *Aerospace*, vol. 10, no. 366, pp. 1–19, 2023.

[4] C. Niephaus, M. Kretschmer, and G. Ghinea, "Qos provisioning in converged satellite and terrestrial networks: A survey of the state-of-the-art," *IEEE Communications Surveys & Tutorials*, vol. 18, no. 14, pp. 2415 – 2441, 2016.

[5] M. Alodeh, S. Chatzinotas, and B. Ottersten, "User Selection for Symbol-Level Multigroup Multicasting Precoding in the Downlink of MISO Channels," in *2018 IEEE International Conference on Communications (ICC)*, May 2018.

[6] A. Bandi, B. S. Mysore R, S. Maleki, S. Chatzinotas, and B. Ottersten, "A Novel Approach to Joint User Selection and Precoding for Multiuser MISO Downlink Channels," in *2018 IEEE Global Conference on Signal and Information Processing (GlobalSIP)*, Nov 2018, pp. 206–210.

[7] A. Bandi, B. Shankar M. R, S. Chatzinotas, and B. Ottersten, "A Joint Solution for Scheduling and Precoding in Multiuser MISO Downlink Channels," *IEEE Transactions on Wireless Communications*, vol. 19, no. 1, pp. 475–490, Jan 2020.

[8] B. Hamet, T. Kolb, C. Rohde, F. Leschka, M. U. Pavan Bhave and, and A. Lidde, "Over-the-Air Operation of Mobile and Multicast Linear Precoding for a Multi-Spot-Beam Mobile Satellite Service ," in *24th Ka and Broadband Communications Conference*, Oct 2018.

[9] B. Hamet, C. Rohde, P. Bhave, and A. Liddell, "Over-the-air Field Trials of Linear Precoding for Multi-spot-beam Satellite Systems," in *22th Ka and Broadband Communications Conference*, Oct 2016.

[10] K. Storek, R. T. Schwarz, and A. Knopp, "Multi-Satellite Multi-User MIMO Precoding: Testbed and Field Trial," in *ICC 2020 - 2020 IEEE International Conference on Communications (ICC)*, June 2020, pp. 1–7.

[11] J. Krivochiza, J. C. M. Duncan, J. Querol, N. Maturo, L. M. Marrero, S. Andrenacci, J. Krause, and S. Chatzinotas, "End-to-end Precoding Validation over a Live GEO Satellite Forward Link," *IEEE Access*, pp. 1–1, 2021.

[12] L. M. Marrero, J. Duncan, J. Querol, N. Maturo, J. Krivochiza, S. Chatzinotas, and B. Ottersten, "Differential Phase Compensation in Over-the-air Precoding Test-bed for a Multi-beam Satellite," in *2022 IEEE Wireless Communications and Networking Conference (WCNC)*, 2022, pp. 1325–1330.

[13] ETSI, "Digital Video Broadcasting (DVB); Second generation framing structure, channel coding and modulation systems for Broadcasting, Interactive Services, News Gathering and other broadband satellite applications; Part 2: DVB-S2 Extensions (DVB-S2X)," 2015.

[14] L. Shan and R. Miura, "Energy-Efficient Scheduling under Hard Delay Constraints for Multi-User MIMO System," in *2014 International Symposium on Wireless Personal Multimedia Communications (WPMC)*, Sep. 2014, pp. 696–699.

[15] M. A. Vàzquez, M. R. B. Shankar, C. I. Kourogiorgas, P. Arapoglou, V. Icolari, S. Chatzinotas, A. D. Panagopoulos, and A. I. Pérez-Neira, "Precoding, Scheduling, and Link Adaptation in Mobile Interactive Multibeam Satellite Systems," *IEEE Journal on Selected Areas in Communications*, vol. 36, no. 5, pp. 971–980, May 2018.

[16] T. Y. Elganimi and F. F. Alfitouri, "Norm-based user selection algorithm for single-RF space modulation techniques with geometric mean decomposition based precoding scheme," *SN Applied Sciences*, vol. 3, no. 1, Jan. 2021.

[17] F. Liu, Y. Zhang, D. Li, and R. Du, "THP-UO algorithm for multi-user mmWave MIMO systems," *Wireless Personal Communications*, vol. 119, no. 3, pp. 2055–2068, Mar. 2021.

[18] J. Krivochiza, J. C. Merlano-Duncan, S. Chatzinotas, and B. Ottersten, "M-QAM Modulation Symbol-Level Precoding for Power Minimization: Closed-Form Solution," in *2019 16th International Symposium on Wireless Communication Systems (ISWCS)*, Aug 2019, pp. 395–399.

[19] R. Bro and S. De Jong, "A Fast Non-negativity-constrained Least Squares Algorithm," *Journal of Chemometrics*, vol. 11, no. 5, pp. 393–401, 1997.

[20] M. Alodeh, S. Chatzinotas, and B. Ottersten, "Symbol-Level Multiuser MISO Precoding for Multi-Level Adaptive Modulation," *IEEE Transactions on Wireless Communications*, vol. 16, no. 8, pp. 5511–5524, Aug 2017.

[21] S. Andrenacci, D. Spano, D. Christopoulos, S. Chatzinotas, J. Krause, and B. Ottersten, "Optimized Link Adaptation for DVB-S2X Precoded Waveforms Based on SNIR Estimation," in *2016 50th Asilomar Conference on Signals, Systems and Computers*, Nov 2016, pp. 502–506.

[22] ETSI, "Digital Video Broadcasting (DVB); Implementation guidelines for the second generation system for Broadcasting, Interactive Services, News Gathering and other broadband satellite applications; Part 1: DVB-S2," 2015.

[23] S. Banerjee, *Linear Algebra and Matrix Analysis for Statistics (Texts in Statistical Science)*. Chapman and Hall, jun 2014.